Efficient Algorithms to Enhance the Audio Signal Management of Unmanned Aerial Vehicles (UAVs)

Jana Alaslani, Scott Bender, Rahul Donnaganti, and Anupama Kar

Final Project Report
Subject: Numerical Linear Algebra for Engineers, MA532
Instructor: Dr. Sirani Mututhanthrige Perera
Semester: Fall 2024
University: Embry-Riddle Aeronautical University

Abstract

Unmanned Aerial Vehicles (UAVs) generate acoustic signals that pose challenges for effective noise reduction. This paper proposes advanced methodologies for modeling, compressing, and minimizing UAV noise, leveraging Singular Value Decomposition (SVD) and its variants, as well as Short-Time Fourier Transform (STFT) analysis. Nonlinear approaches were adopted to improve modeling accuracy, addressing the inherent nonlinear characteristics of UAV noise. These characteristics include the quadratic relationship of intensity and the logarithmic scaling associated with human perception. Randomized SVD (rSVD) was used for efficient noise compression, notably reducing data dimensionality, yet retaining essential frequency-domain attributes. Analysis comparing randomized, truncated, and full SVD, demonstrated rSVD's computational and memory efficiency, with results revealing adequate noise compression for human perception at 15 dB Signal-to Noise Ratio (SNR). Furthermore, static disruptive noise cancellation techniques were employed, displaying limitations in evaluating dynamically changing phase shifts innate in UAV noise. Adaptive methodologies remain required for effective noise reduction, despite the inefficiency in cases with rapid phase variation within static noise

1 Introduction

Unmanned Aerial Vehicles (UAVs), often referred to as "drones," have become an integral part of modern technology and are expected to experience tremendous growth. Consequently, they are a significant source of environmental noise pollution. The increasing UAV operations have raised concerns about their impact on human annoyance and well-being, necessitating the development of legislation and standardization [1]. According to the ANSI Standardization Roadmap of 2020, there are currently no identified standards for drone noise; however, further research into acoustical features is necessary to address these shortcomings [2]. The first step is identifying the target, noise, and distinguishing it from sound. Sound is a general term that describes mechanical radiant energy transmitted through a medium via longitudinal wave movement and is the primary objective cause of hearing. Noise, on the other hand, refers specifically to sounds that are unwelcome, disruptive, or harmful. This paper focuses on mitigating such noise. [3].

Established methods for analyzing UAV noise often assume linear sound propagation. While these methods simplify sound modeling, they fail to account for nonlinear patterns caused by environmental disruptions and human auditory processing [4].

Fast Fourier Transform (FFT) is a widely used computational algorithm that efficiently calculates Fourier coefficients, significantly reducing computational load for digital spectral analysis and filter simulation. It is fundamental in signal analysis in both the time and frequency domains. The origins of FFT can be traced back to Carl Friedrich Gauss's attempts to compute asteroid orbits, which led to the development of the Discrete Fourier Transform (DFT) matrix. Subsequently, the Cooley-Tukey algorithm further generalized and optimized this method [5]. FFT computes the DFT matrix and its inverse, IDFT, for a sequence. Direct computation of NxN DFT for large datasets is computationally expensive; FFT addresses this by reusing repetitive calculations, reducing computational complexity from $O(N^2)$ to $O(N \log N)$ [6].

Another widely utilized method for signal processing is Power Spectral Density (PSD). It provides a statistical representation of a signal's power distribution across various frequencies, offering insights into frequency-dependent variations in signal strength [7]. While FFT delivers detailed frequency spectra, PSD identifies dominant frequencies and analyzes power features. Together, they are essential for signal analysis. However, FFT combined with PSD is more effective for stationary signals, struggling with non-stationary noise [8]. Time-frequency analysis methods, such as Short-Term Fourier Transform (STFT) or wavelet transforms, provide more accurate insights for analyzing the time-varying frequency content of non-stationary signals.

Least Mean Square (LMS) is yet another prominent method for audio signal processing and noise cancellation. LMS is an adaptive filtering algorithm that extracts noise from an input signal. Unlike traditional static filters, adaptive filtering tracks wide-spectrum signals, making it ideal for noise reduction [9]. Real-time LMS implementations have proven effective in reducing noise but face challenges when addressing narrowband non-periodic noise [10].

This paper proposes an alternate algorithm combining STFT and Randomized Singular Value Decomposition (rSVD). STFT changes the time domain data into frequency data and Randomized SVD provides a low rank approximation of the data to identify the most efficient noise mitigation technique. The study uses UAV noise data from NASA's DELIVER project, provided by Stephen A. Rizzi and Andrew W. Christian, to analyze human responses to noise sources such as small Unmanned Aerial Systems (sUAS) and road vehicles. Using data from the DELIVER Psychoacoustic Test (WGA-I) Database [11], the algorithm is tested.

The contributions and organization of this paper are as follows:

- **Section 2** discusses efficient noise compression techniques using SVD variants for computationally efficient low-rank approximations of UAV noise data. Additionally, time and frequency domain analysis is conducted using STFT to identify dominant noise patterns. Finally, the practicability of disruptive noise cancellation is evaluated, highlighting the limitations of static techniques under rapidly varying phase shifts.
- **Section 3** evaluates UAV noise compression using SVD variants, focusing on computational efficiency and accuracy through metrics such as Mean Squared Error (MSE) and Signal-to-Noise Ratio (SNR). The efficacy of static disruptive noise cancellation is examined, including the impact of a 135 Hz Notch filter, with a detailed performance assessment.

- **Section 4** addresses increasing noise complaints related to UAVs and other vehicles, emphasizing the growth of UAV usage and the necessity of audio signal management techniques in various fields. The section also explores potential applications of the proposed algorithm in swarm drone technology for enhanced efficiency and comprehensive data collection.
- **Section 5** concludes the paper by summarizing the advantages of the proposed algorithm compared to current methods, presenting the results of SVD variant comparisons, and discussing key outcomes of noise cancellation.
- **Section 6** presents future work relevant to this paper including adding another layer of analysis into the algorithm provided, experimenting with techniques previously implemented, and expanding on the comparative aspect of the report.

2 Methodology

2.1 Linear vs Non-Linear Modeling

UAV audio data exhibits inherent nonlinearity due to a combination of physical, environmental, and perceptual factors. As UAV-generated audio propagates through the air, it follows the inverse-square law, causing sound intensity to decrease nonlinearly with distance. Additionally, sound pressure and intensity display a quadratic relationship, while environmental effects such as reflections, interference, and absorption distort sound waves in unpredictable ways. Human perception introduces another layer of nonlinearity, as sound intensity is processed logarithmically on the decibel (dB) scale. Therefore, effectively modeling UAV audio data requires a nonlinear approach to account for these intricate characteristics [12].

2.2 UAV Audio Compression Techniques Utilizing SVD Variants

Noise compression is essential in sound processing, particularly for UAVs, which generate complex acoustic signals filled with noise from various sources. These sound signals often contain critical information, including distinct acoustic events or operational indicators, but they also contain redundant data that can hinder storage and analysis efficiency. Therefore, Singular Value SVD, both in its standard and randomized forms, provides a robust solution for noise compression where efficiency and clarity are crucial. This section compares traditional SVD approaches with randomized SVD to evaluate its computational efficiency and accuracy in processing large-scale acoustic data.

2.2.1 Noise Compression Utilizing SVD

After obtaining the matrices A_i (representing either time-domain signals or frequency-domain representations such as spectrograms) from multiple data files, the matrices for all i UAVs are concatenated into a composite matrix A.

$$A = \begin{bmatrix} A_1 & A_2 & \dots & A_i \end{bmatrix}_{m \times n} \tag{1}$$

SVD is then applied to the composite matrix A [13]

$$A = U\Sigma V^T \tag{2}$$

where $U \in \mathbb{R}^{m\times m}$ is an orthogonal matrix of left singular vectors, $\Sigma \in \mathbb{R}^{m\times n}$ is a diagonal matrix of singular values σ_i, and $V^T \in \mathbb{R}^{n\times n}$ is an orthogonal matrix of right singular vectors. Note that the singular values are sorted such that $\sigma_1 \geq \sigma_2 \geq \cdots \geq \sigma_r$, where r is the rank of the composite matrix A ($r = \text{rank}(A)$).

The left singular vectors in U capture the dominant modes in the rows of A, corresponding to either frequency for frequency-domain data or temporal variations for time-domain data. The singular values σ_i represent the contribution of each mode to the composite matrix A, and the right singular vectors in V^T provide the associated patterns along the columns of A, reflecting temporal or spatial variability.

The matrix A can be reconstructed as:

$$A = \sum_{i=1}^{r} \sigma_i \vec{u}_i \vec{v}_i^T \tag{3}$$

where u_i is the i-th column of U, indicating the spectral content of mode i, and v_i^T is the i-th row of V^T, indicating the temporal pattern of mode i.

The dominant patterns or modes are then identified by examining the singular values σ_i, which quantify the energy contribution of each mode. To find the significance of a specific component, such as f_k for the frequency domain, u_i is projected onto the corresponding axis and computed as follows:

$$f_k = |u_{i,k}|\, \sigma_i \tag{4}$$

where $u_{i,k}$ is the k-th entry of the i-th singular vector u_i.

Matrix A is then approximated by retaining only the first P dominant singular values:

$$A_p = \sum_{i=1}^{p} \sigma_i \vec{u}_i \vec{v}_i^T \tag{5}$$

resulting in peak frequencies with noise filtration.

2.2.2 Noise Compression Utilizing Randomized SVD

rSVD is a variant of SVD designed to accelerate SVD computations on large matrices. UAV sound data is often represented as a large matrix because it captures acoustic signals over an extended time frame. The process records a high number of data points per second, resulting in a substantial volume of information. Randomized SVD accelerates these computations by first transforming the original matrix into a lower-dimensional subspace while still preserving its key features. This dimensionality reduction makes performing full SVD or economical SVD faster and less computationally intensive.

Randomized SVD can be performed in either the time domain or frequency domain, depending on the

analysis requirements. The primary difference lies in the input format. In the time domain, the input is a large column vector of size $mn \times 1$, which must be reshaped into a matrix A, where $A \in \mathbb{R}^{m \times n}$, before applying randomized SVD. In the frequency domain, as discussed later in this report, the output of a STFT is already in the form of a matrix A, where $A \in \mathbb{R}^{m \times n}$, eliminating the need for reshaping prior to performing randomized SVD. The steps for performing randomized SVD are as follows:

1. Random Projection
   The randomized SVD approach begins by projecting matrix A onto a lower-dimensional subspace. This is done by creating a random matrix Ω with entries drawn from a standard Gaussian distribution (mean 0 and variance 1). By multiplying A with Ω, we obtain a matrix Y that captures the key features of A.

   $$Y = A\,\Omega \tag{6}$$

   where $A \in \mathbb{R}^{m \times n}$, $\Omega \in \mathbb{R}^{n \times k}$, and $Y \in \mathbb{R}^{m \times k}$.

2. QR Decomposition
   QR decomposition factors matrix Y into an orthogonal matrix Q and an upper triangular matrix R. This step is crucial to ensure numerical stability; omitting it would make the algorithm computationally faster, but could lead to accumulated errors.

   $$Y = QR \tag{7}$$

   where $Q \in \mathbb{R}^{m \times k}$ and $R \in \mathbb{R}^{k \times k}$.

   To achieve this factorization, the Householder reflections method is employed to iteratively transform Y while maintaining numerical stability. A Householder reflection is a transformation that zeros out the elements below the diagonal of the matrix Y. The reflection matrix H is defined as:

   $$H_j = I - 2\frac{\vec{u}_j \vec{u}_j^T}{\vec{u}_j^T \vec{u}_j}, \tag{8}$$

   where $\vec{u}_j = Y_{i,j} + \text{sign}(Y_{j,j})\|Y_{i,j}\|\vec{e}_j$.
   The orthogonal matrix Q^T is computed as:

   $$Q^T = H_1 H_2 \cdots H_k. \tag{9}$$

   Here, Q has orthonormal columns and spans the same subspace as Y. The matrix Q is essential because it enables working with a smaller matrix while preserving the key information of A. Since the triangular matrix R is not relevant to randomized SVD, it does not need to be computed.

3. Projection onto the Subspace Defined by Q
   Matrix A is projected onto the subspace defined by Q:

   $$B = Q^T A, \tag{10}$$

   where $B \in \mathbb{R}^{k \times n}$.

The matrix B is significantly smaller than the original matrix A, assuming $k \ll m, n$. This reduced matrix B captures the essential information of the original matrix A. Singular Value Decomposition (SVD) can then be performed on B to obtain the leading singular values.

4. Economical SVD on the Smaller Matrix B

   The economical SVD of B is represented as:

$$B = \tilde{V}\Sigma V^T, \tag{11}$$

   where $\tilde{V} \in \mathbb{R}^{k\times k}$, $\Sigma \in \mathbb{R}^{k\times k}$, and $V \in \mathbb{R}^{n\times k}$.

   Here, $\tilde{V}$ is an orthogonal matrix containing the left singular vectors of B, while V is an orthogonal matrix containing the right singular vectors of B. The diagonal matrix Σ contains the singular values of B, sorted in descending order, which represent the importance of the corresponding singular vectors.

5. Obtaining the low rank approximation of Matrix A

   The low-rank approximation of matrix A is given by:

$$A_{\mathrm{p}} = Q\tilde{U}\Sigma V^T. \tag{12}$$

   Randomized SVD can be applied in the frequency domain of spectrograms to create a low-rank approximation of the audio signal [14]. By performing this decomposition, the essential frequency-domain features of the audio file are preserved while reducing the dimensionality of the data. This low-rank approximation serves as a compact representation, significantly improving computational efficiency.

   This algorithm can be used as part of noise minimization processes. Despite the reduced data size, the approximation retains sufficient information to effectively minimize noise, striking a balance between computational speed and performance.

2.3 UAV Noise Minimization

2.3.1 Low Rank Frequency Domain Approximation Utilizing STFT and rSVD

Generally, MATLAB's built-in Cooley-Tukey Radix-2 FFT algorithm is used for active noise cancellation. Initially, a regular FFT was attempted. However, a significant limitation was observed: the regular FFT provides the frequency profile of a UAV data file, but does not show the evolution of these profiles over time. The signals are not periodically continuous over an infinite duration, offering only a static profile that fails to represent dynamic changes. This lack of a smooth profile is due to spectral leakage. To address this issue, the STFT (Short-Time Fourier Transform) algorithm was chosen.

The STFT algorithm uses a small, predefined window $\vec{w}(n)$ and processes the entire input vector through that window. This way, the whole signal is "windowed" into smaller segments, and FFT is applied to each segment to compute the STFT matrix. The process involves the following steps: 1. Windowing, 2. Sliding the window, 3. Applying the window, 4. Computing the Fourier Transform (DFT), and 5. Obtaining the STFT output.

Windowing is essential for efficient STFT application. A key requirement for any FFT is that the time-domain signal should exist infinitely. For periodic signals, this is not an issue. However, the UAV sound data utilized is non-periodic. To avoid spectral leakage and attain a pure tone in the frequency domain, a Hamming window is used [15]. Since audio files vary in length, they are trimmed to the minimum length among all files. The window size for the STFT is set to 4096 to capture high-resolution frequency changes.

The sliding window is managed by the overlap command. After every 4096 elements are processed, the window slides to the next set with an overlap of 3072 to ensure high-resolution results. Greater overlap results in a smoother signal for further processing. After applying the window, FFT is computed over these small windows with $nfft$ transforms done overall. The FFT of the sequence $x[n]$ of length N is defined as:

$$\vec{X}[k] = \sum_{n=0}^{N-1} \vec{x}[n] e^{-i2\pi kn/N}, \tag{13}$$

where: $\vec{X}[k]$ is the frequency matrix, k ranges from 0 to $N-1$, i is the imaginary unit, and $\vec{x}[n]$ is the time-domain signal [16].

The output of this process is a set of matrices A_1, A_2, A_3. The STFT command generates a matrix. This is because for each segment, the command creates a column vector and concatenates all these column vectors to form a matrix. The flop count of the STFT used here can be given by:

$$\text{Number of windows} \times \text{Flops per FFT} = O\left(\frac{L}{H} \cdot N \log_2 N\right), \tag{14}$$

where: L is the length of the input vector (`minLength`), H is the hop size (`windowSize` minus the overlap), and N is the FFT size (`nfft`).

The outputs A_1, A_2, A_3 are concatenated and fed into the compression algorithm to create a low-rank approximation of the spectrograms. Based on the comparison shown in Section 3, randomized SVD is computationally efficient and provides the necessary accuracy for analysis. Thus, randomized SVD is applied to the matrices A_1, A_2, A_3.

2.3.2 Disruptive Noise Canceling

Let the position of the UAV be represented by:

$$\vec{r}_{\text{UAV}} = (x_{\text{UAV}}, y_{\text{UAV}}, z_{\text{UAV}}). \tag{15}$$

The distance between the UAV and the receiver is computed by taking the 2-norm of $\vec{r}$:

$$\|\vec{r}\|_2 = \sqrt{(-x_{\text{UAV}})^2 + (-y_{\text{UAV}})^2 + (-z_{\text{UAV}})^2} = \sqrt{(x_{\text{UAV}})^2 + (y_{\text{UAV}})^2 + (z_{\text{UAV}})^2}. \tag{16}$$

The sound intensity, I, follows the inverse square law, which is represented as:

$$I \propto \frac{A}{\|\vec{r}\|_2^2}, \tag{17}$$

where A represents the amplitude of the sound wave.

Using this information, along with the generated amplitude of the sound wave as a function of time, a 3D predictive model of sound intensity can be developed. This model provides a detailed visualization of how noise propagates in space from the UAV to the receiver at any location. It demonstrates the variation in intensity as a function of distance and position relative to the UAV's trajectory, as presented in Figure 1.

From the model, it is evident that the highest amplitude occurs between 10 and 15 seconds for each UAV sound file. Furthermore, this model can identify problem areas where the UAV generates high-intensity noise. These problem areas are locations where the noise minimization algorithm can be applied to effectively reduce the intensity of the perceived noise.

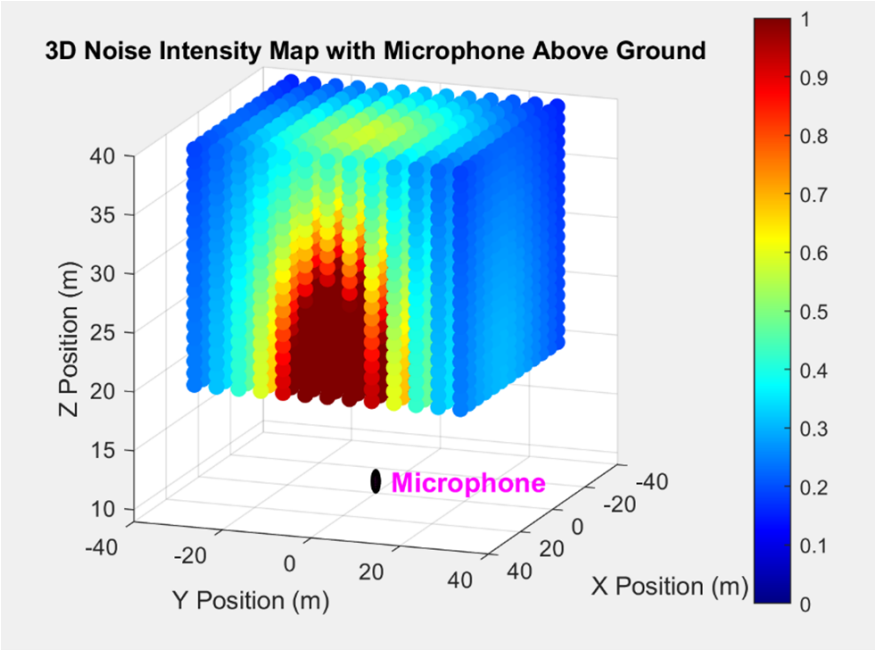

Figure 1: Location of noise pollution intensity relative to a microphone representing a bystander.

To apply disruptive noise cancellation and eliminate a dominant frequency, it is essential to identify how the phase of that frequency changes with respect to time. Only frequencies with predictable phase changes are suitable candidates for this noise cancellation technique. For active noise-canceling headphones, various filtering methods and algorithms are applied to rapidly identify and predict dominant frequency ranges and phase changes [17].

In this research, the feasibility of static disruptive noise cancellation was explored. This process involved:

1. Identifying a dominant frequency present across all three UAV sound files,
2. Generating a disruptive sound signal with the same frequency but with a phase offset by 180 degrees and equal amplitude, the impact of phase shift on signal attenuation is presented in Figure 2.

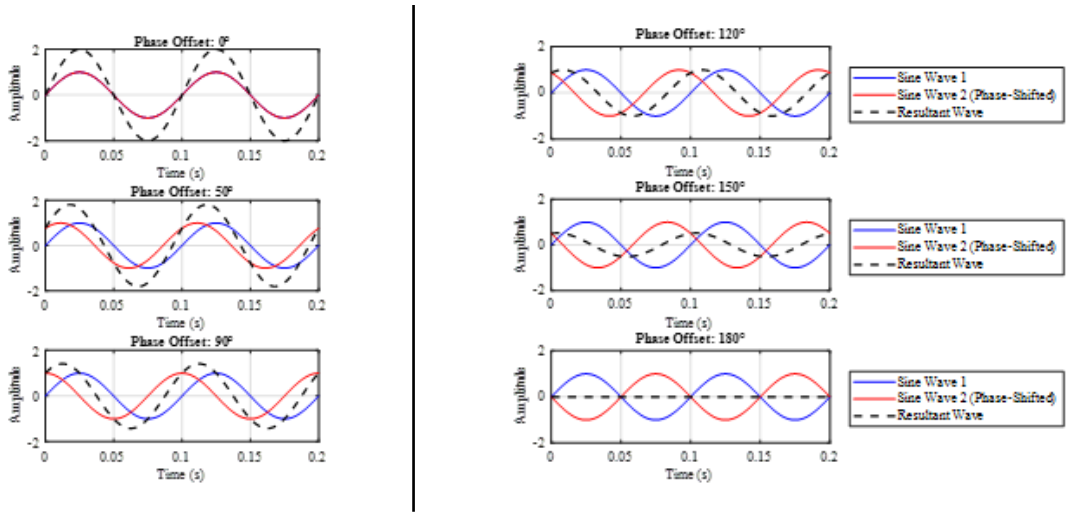

Figure 2: The effect of Phase shift on attenuating a signal wave using a disruptive wave of equal frequency and amplitude.

Additionally, only frequencies with phases that change very slowly and are easily predictable were considered for this noise cancellation methodology. Dominant frequencies below 250 Hz were evaluated during the 5-second interval when UAV noise intensity was the highest. This evaluation was conducted by analyzing the resulting STFT for each signal using MATLAB.

After identifying the most dominant frequency across all signals, the phase for each signal was evaluated to determine how the phase of the dominant frequency was changing. This analysis provided a basis for assessing the feasibility of introducing static noise cancellation to reduce UAV noise pollution.

Finally, the impact of eliminating the dominant frequency was evaluated using a Notch filter applied to the original signals.

3 Numerical Results

3.1 Audio Compression Utilizing SVD Variants

To evaluate the rank approximation for the audio data, two key performance metrics are used: Mean Squared Error (MSE) and Signal-to-Noise Ratio (SNR). These metrics quantify the low-rank approximation by determining how closely the approximation captures the original data. When paired with computational efficiency, these metrics allow for evaluating the trade-offs between computation time and approximation accuracy.

MSE is a fundamental metric that quantifies the average squared disparity between the original signal and its approximated counterpart. In this context, it measures how well the low-rank approximation preserves the essence of the original audio data. MSE is calculated using the following formula:

$$\text{MSE} = \frac{1}{N}\sum_{i=1}^{N}(A - A_{\text{p}})^2, \tag{18}$$

SNR measures how much of the original signal's essence remains intact compared to the unwanted noise introduced during the low-rank approximation. A higher SNR indicates a clearer, more accurate representation of the original signal, while a lower SNR suggests that some attributes of the original signal have been lost. The SNR is calculated using the following formula:

$$\text{SNR} = 10 \log \left(\frac{\frac{1}{N} \sum_{i=1}^{N} A^2}{\text{MSE}} \right). \tag{19}$$

Singular Value Decomposition (SVD), Truncated SVD, and Randomized SVD were performed in the time domain on an audio file, with rank values varying between 1 and 1000. The performance of each method was evaluated based on computation time, Mean Squared Error (MSE), and Signal-to-Noise Ratio (SNR), with the results visualized in the graph below. Using these performance metrics, the optimal rank value that minimizes MSE - while balancing SNR and computational efficiency - was determined for each method.

The findings are summarized in Figure 3 below, with the corresponding MATLAB script in Appendix C, Listing 1.

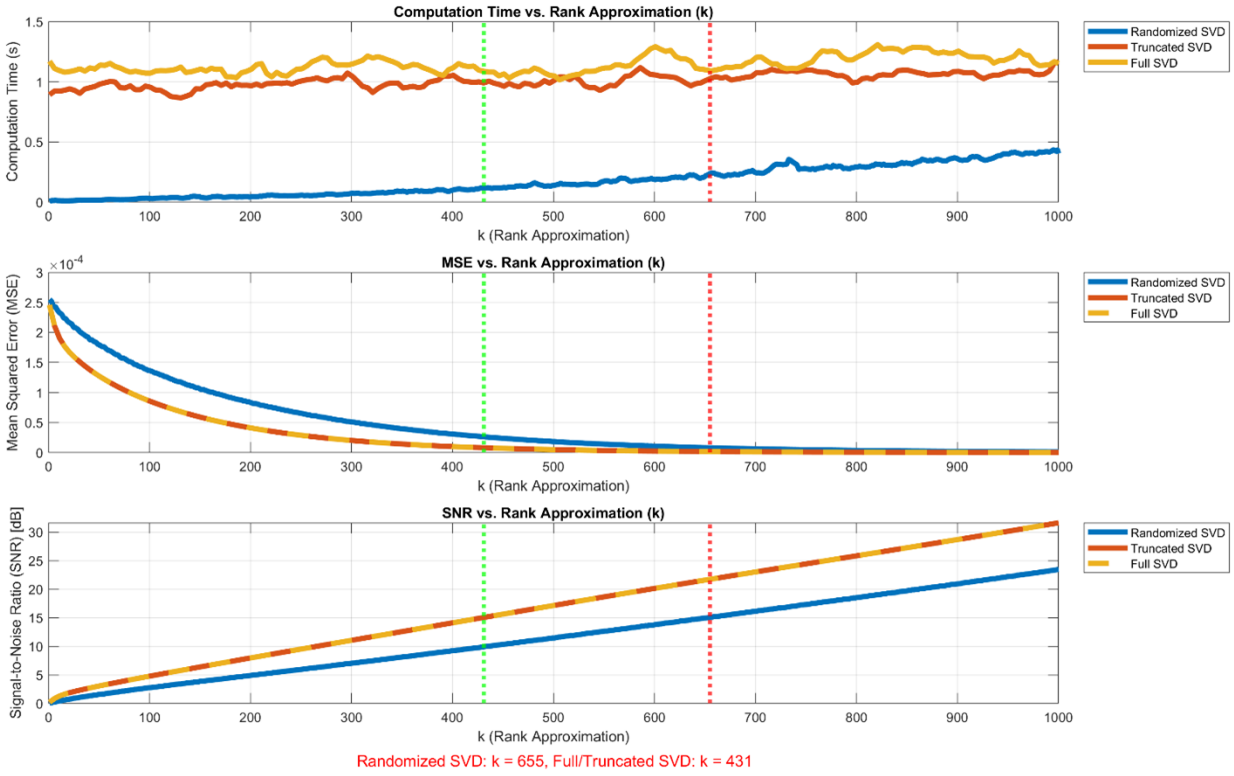

Figure 3: Evaluation of the Computation time, Mean Squared Error, and Signal-to-Noise Ratio of Randomized SVD, Truncated SVD, and Full SVD.

To effectively choose a rank value to perform the low rank approximation, an SNR cutoff of 15 dB is used. At this SNR value, UAV noise compression is driven by the focus on human perception, rather than the preservation of the UAV sound's finer acoustic details. This SNR level provides a balance between retaining

sufficient signal fidelity for audibility and suppressing excess redundant noise, thereby ensuring computational efficiency without compromising the relevance of the data for perception studies. Additionally, this choice avoids over-preservation of acoustic details, such as rotor harmonics, which are not critical for the intended study. By targeting 15 dB, the analysis aligns with environmental noise standards and achieves a practical balance between quality and efficiency, making it ideal for public perception. Table 1, shown below, presents the performance metrics for various SVD forms, highlighting the algorithms' effectiveness and efficiency.

Table 1: Comparison of SVD methods based on performance metrics.

Method	**Time (s)**	**Flop Count**	**SNR (dB)**	**MSE**	**Rank (k)**
Randomized SVD	0.3369	$O(mnk) + O(nk^2)$	15.08	0.000008	655
Truncated SVD	0.8905	$O(mn \cdot \min(m, n))$	15.05	0.000008	431
Full SVD	0.9259	$O(n^2m + m^2n)$	15.05	0.000008	431

For randomized SVD, the total flop count is represented as a combination of precomputation and post-computation. Assuming $k \ll n$, the flop count is expressed as:

$$O(mnk) + O(nk^2), \tag{20}$$

where the first term corresponds to precomputation and the second term corresponds to post-computation.

For truncated SVD, also known as economical SVD, the flop count is represented as:

$$O(mn \cdot \min(m, n)). \tag{21}$$

In terms of memory cost, truncated SVD requires $O(2k)$ passes over the matrix A, whereas randomized SVD requires only 2 passes over A, regardless of the chosen k value. This makes randomized SVD more memory-efficient compared to truncated SVD.

The analysis shown in Figure 4 demonstrates the effectiveness of the randomized SVD algorithm for compressing and reconstructing sound data associated with various UAV trajectories. The corresponding MATLAB script can be found in Appendix C, Listing 2. Applying the algorithm to sound datasets from multiple flight paths and multiple UAVs, the reconstructed sound files closely align with the original recordings. These visualizations highlight the algorithm's robustness and consistency across various trajectory patterns, confirming its general applicability to UAV related sound data. This validates the use of the randomized SVD technique as a reliable method for efficient sound data compression without significant loss of fidelity.

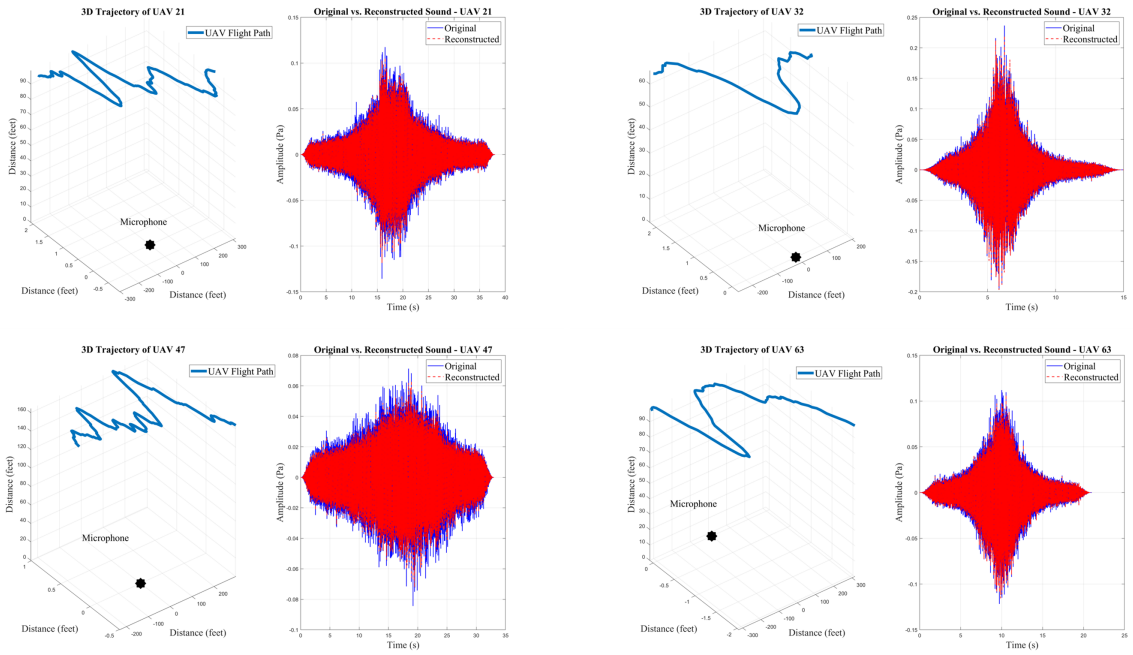

Figure 4: Effectiveness of SVD-based noise reduction on various UAV trajectories.

3.2 Static Disruptive Noise Cancellation

Considering the effectiveness of randomized SVD in providing a reduced-rank approximation of the UAV noise data, this approach will be continued. To evaluate its effectiveness, a spectrogram was developed comparing the original signal to a reconstructed spectrogram after applying randomized SVD with a rank of 655.

Additionally, the amplitude in dB is plotted for both the original and reconstructed signals. These comparisons are presented in Figure 5, with the corresponding MATLAB scripts in Appendix C, Listing 3 and 4.

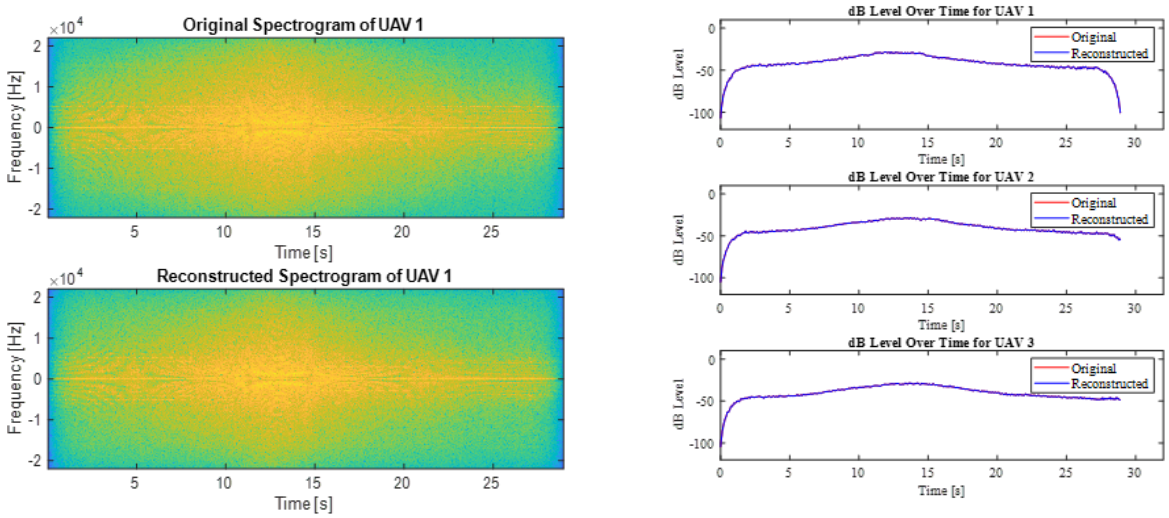

Figure 5: Spectrogram of UAV 1 before and after applying Randomized SVD with a Rank of 655 (Left) and a comparison of the change in dB Levels from these reconstructed signals for each UAV (Right).

Analyzing the dominant frequencies below 250 Hz across all UAV sound files revealed that the frequency of 135 Hz produced the largest decibel change in all three sound files. Based on this finding, a preliminary analysis was conducted using a Notch filter to eliminate the 135 Hz frequency from the UAV noise data, as presented in Figure 6.The corresponding MATLAB script can be found in Appendix C, Listing 5.

From this analysis, it was observed that reducing this low frequency did not significantly decrease the overall amplitude of the UAV noise data. Additionally, the phase change was evaluated over the 5-second interval with the loudest noise, also shown in Figure 6. This assessment demonstrates that the phase, while changing almost linearly, varies significantly during this time step, ranging from 0 radians to over 200 radians. This variability in phase complicates the use of a generic static noise frequency for multiple cases. It would be highly improbable to align the phase correctly without employing adaptive filtering techniques.

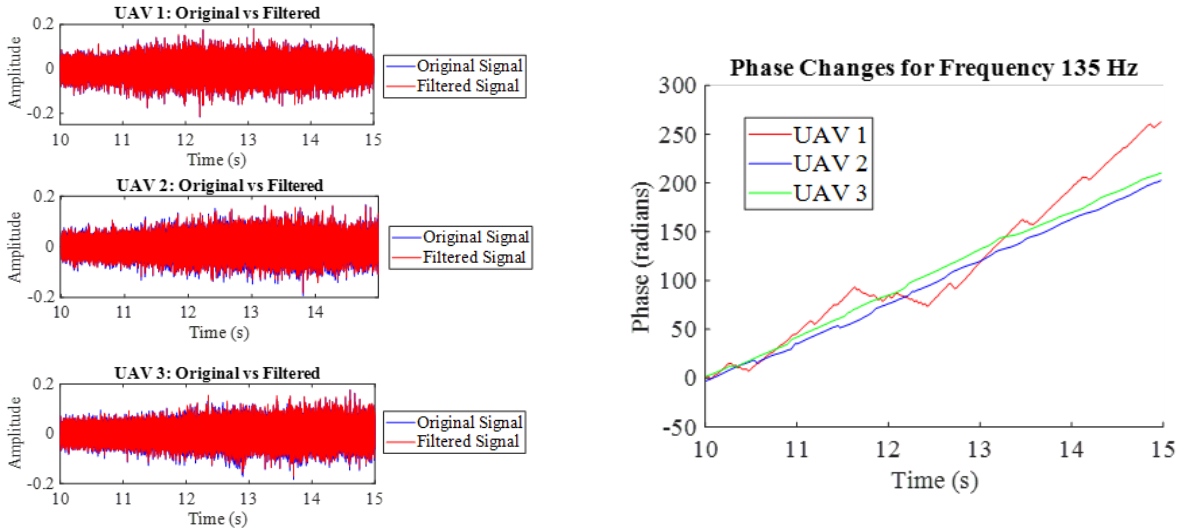

Figure 6: UAV Noise Pollution with 135 Hz frequency filtered using a Notch Filter (left) and evaluation of how the phase of the dominant frequency (135 Hz) changes for each UAV (right).

A demonstration in which UAV noise, with a changing phase shift of 2400 radians per minute, is attenuated using a static disruptive signal of equal amplitude, is presented in Figure 7. After combining the static disruptive wave signal with the UAV noise, the resultant wave has a greater amplitude.

This observation highlights that when applying static noise cancellation to a signal with a rapidly changing phase, the resultant signal will increase in amplitude. Therefore, in the case of UAV noise pollution cancellation, the noise will increase rather than be attenuated.

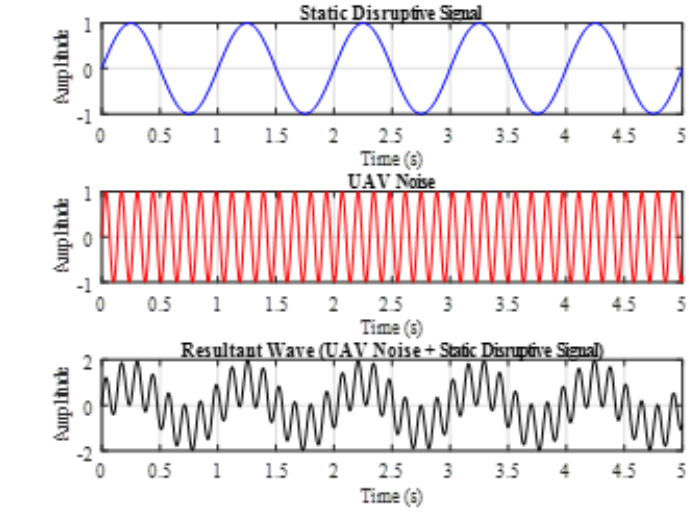

Figure 7: The effect of static noise disruption on UAV noise.

Considering the ideal case where UAV noise pollution occurs under known conditions with known phase shifts, such as the audio files used in this report, it is plausible to generate a disruptive signal capable

of completely eliminating the noise.

To evaluate this, randomized SVD was utilized with a rank of 655 to compress the signal. Using the Short-Time Fourier Transform (STFT), MATLAB was employed to generate a disruptive signal. The resultant signal, after applying the generated disruptive signal, is compared to the original signal in Figure 8.

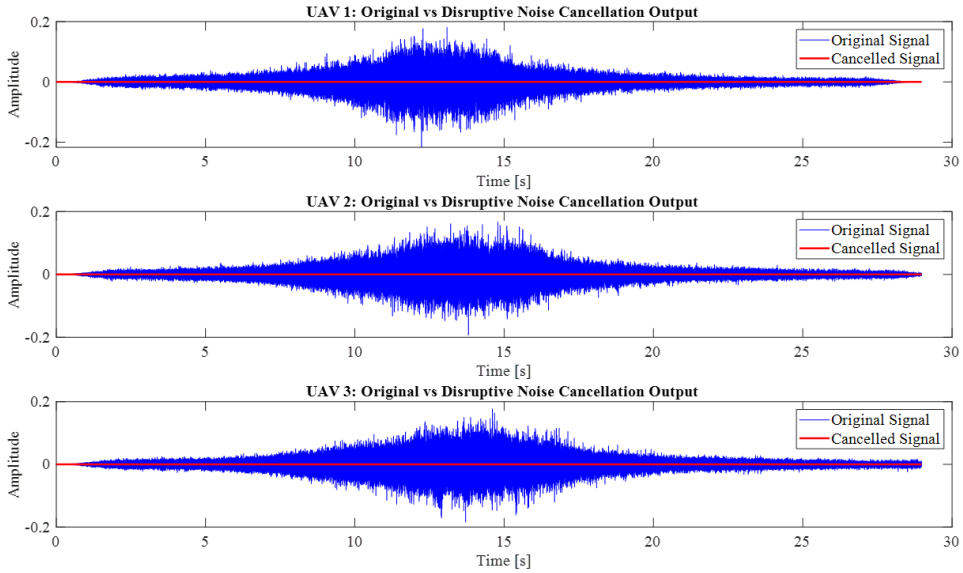

Figure 8: Known UAV Noise Pollution canceled using disruptive noise cancellation after compressing the signal using randomized SVD with a rank of 655.

3.3 Precision and Performance in Computational System

The hardware and software used for computations are presented below in Table 2. Based on the specifications, the computational system is robust and capable of performing calculations in both single and double precision.

Although double precision requires more computational time and storage, it improves the accuracy of computations. Additionally, MATLAB's core functions and operations are optimized for double precision. Enforcing single precision may lead to unexpected behavior or compatibility issues.

There are no concerns with overflow or underflow since all values used in the computations remain within the bounds of the minimum and maximum positive values.

Table 2: Hardware and Software Specifications

Laptop Model:	Dell XPS 16
Processor:	Intel Core Ultra 9 185H, 2.5 GHz, 8 cores, 16 threads, 64-bit architecture
GPU(s):	Intel(R) Arc(TM) Graphics and NVIDIA RTX 4070
RAM:	64 GB DDR5
Storage:	1 TB NVMe SSD
Operating System:	Windows 11 Version 23H2
MATLAB Version:	MATLAB R2024b
Execution Mode:	Double precision
Minimum Positive Value:	2.2251×10^{-308}
Maximum Positive Value:	1.7977×10^{308}
Machine Precision (δ):	2.2204×10^{-16}

4 Applications

In the first nine months of 2024, Florida received 814 noise complaints, including those related to UAVs, as reported by the FAA's Aviation Noise Complaints and Inquiry Response (ANCIR) portal (see Appendix B) [18] . A 2011 Aero News Network article highlighted the severity of noise issues around KDAB and KEVB, quoting a New Smyrna Beach resident who described the noise as "horrendous" and disruptive to everyday activities. With the UAV industry growing and drones flying closer to the ground than any other aircraft, noise complaints are expected to increase rapidly [19]. Similar complaints have been reported for nearby airports like Naples, Lakeland, and Flagler [20] [21] [22]. Florida's favorable weather makes it a popular destination for drone activities and events, further contributing to its status as a noise complaint target and expanding its variable applications.

Trajectory-based noise reduction in drone swarms is an example application to managing noise levels in various operational scenarios. Unlike single drones, swarm drones function collectively, recording and transmitting data across multiple UAV units at the same time stamp. Its application increases efficiency and provides real-time datasets, which is beneficial for environmental observations and disaster responses. By identifying the points along a drone's flight path that generates the most noise and compressing those frequencies, significant noise reduction can be achieved. This universal algorithm, initially designed for handling multiple time-varying trajectories, can be effectively applied to drone swarms. Control inputs are sent to a few key nodes, which then propagate the inputs through the swarm, like a neural network. The described decentralized control system ensures efficient management of the swarm's trajectory and noise levels and the extension of these principles to drone swarms, whether flying in formation (single trajectory) or dispersed (multiple trajectory), demonstrates the adaptability and effectiveness of the noise reduction algorithm. This approach enhances the operational capabilities of drone swarms, making them more efficient, enhancing usability and societal acceptance with quieter, more efficient operations [23].

5 Conclusion

While FFT with PSD efficiently analyzes stationary signals, it struggles with non-stationary noise. The LMS method, though simple and suitable for real-time applications, may also falter with highly non-linear noise. STFT with SVD captures time-frequency information effectively for non-stationary signals. To address the limitations of using solely STFT or SVD, and to accommodate various types of noise signals, the proposed method is recommended. STFT effectively analyzes the frequency domain of noise and sound within a signal, while randomized SVD robustly decomposes and truncates noise. However, applying SVD for active noise cancellation presents challenges due to its matrix-based nature and lack of phase data, making out-of-phase cancellation difficult. Despite these challenges, the combined method shows significant promise for mitigating complex noise environments, particularly in applications like UAV swarm operations, urban noise reduction, and environmental monitoring.

6 Future Work

Finally, although the objective of the paper was achieved, further analysis can be implemented to expand on the limitations and comparison between widely utilized algorithms such as Fast Fourier Transform (FFT), Power Spectral Density (PSD), and Least Mean Square (LSM) with Short-Time Fourier Transform (STFT) and (Singular Value Decomposition (SVD). However, promising future direction for this research involves designing a neural network. Traditional ReLU functions may not be suitable due to their zero derivatives at certain points, which could hinder backpropagation and weights' refinement. Given the nonlinear nature of drone noise, Sigmoid and Tanh functions are more appropriate for structuring the hidden layers and output layer. To enhance the network's training, a bulk of additional data files would be necessary so the network can pass successfully through more epochs during training. Exploring a Convolutional Neural Network (cNN) is an option, but an innovative approach would be to develop a structured Neural Network (strNN). A suggestion is to avoid using the built-in MATLAB's patternnet command, as it inherently creates a single hidden layer by default. This limitation makes it unsuitable if a need arises for multiple hidden layers.

References

[1] S. A. Rizzi and D. L. H. et al., "Urban air mobility noise: Current practice, gaps, and," Online: https://ntrs.nasa.gov/api/citations/20205007433/downloads/NASA-TP-2020-5007433.pdf, NASA, Tech. Rep., 2020.

[2] S. Gössling, C. Schreyer, and R. Zunker, "Drone noise emission characteristics and noise effects on humans—a systematic review," *International Journal of Environmental Research and Public Health*, vol. 18, no. 11, p. 5940, 2021. [Online]. Available: https://www.mdpi.com/1660-4601/18/11/5940

[3] N. Y. C. D. of Environmental Protection, "Sound vs. noise: Distinguishing between sound and noise," n.d. [Online]. Available: https://www.nyc.gov/assets/dep/downloads/pdf/environment/education/l1-sound-noise-distinguishing-sound-noise.pdf

[4] R. Kapoor, N. Kloet, A. Gardi, A. Mohamed, and R. Sabatini, "Sound propagation modelling for manned and unmanned aircraft noise assessment and mitigation: A review," 2021. [Online]. Available: https://www.mdpi.com/2073-4433/12/11/1424

[5] A. Gasmi, "What is fast fourier transform?" *ResearchGate*, 2022. [Online]. Available: https://www.researchgate.net/publication/362419674_What_is_Fast_Fourier_Transform

[6] M. Cerna and A. F. Harvey, "The fundamentals of fft based signal analysis and measurement," 2020. [Online]. Available: https://www.sjsu.edu/people/burford.furman/docs/me120/FFT_tutorial_NI.pdf

[7] R. Acharya, "Satellite signal propagation, impairments and mitigation," *ScienceDirect*, 2017. [Online]. Available: https://www.sciencedirect.com/science/article/pii/B9780128097328000089

[8] Mathworks, "Power spectral density analysis using fft," *MathWorks*, 2020. [Online]. Available: https://www.mathworks.com/help/signal/ug/power-spectral-density-estimates-using-fft.html

[9] P. Diniz, *Adaptive Filtering*. Springer, 2013.

[10] J. Cedarleaf, S. Philbert, and A. Ramanathan, "Noise cancellation using least mean squares adaptive filter," 2017. [Online]. Available: https://hajim.rochester.edu/ece/sites/zduan/teaching/ece472/projects/2017/JonathanCedarleaf_StevePhilbert_ArvindRamanathan_paper.pdf

[11] S. A. Rizzi and A. W. Christian, "Deliver psychoacoustic test database," 2020.

[12] P. Papacosta and N. Linscheid, "The confirmation of the inverse square law using diffraction gratings," *The Physics Teacher*, vol. 52, pp. 243–245, 2014.

[13] B. N. Datta, *Numerical Linear Algebra and Applications*, second edition ed. The Society of Industrial and Applied Mathematics, 2010.

[14] N. Halko, P. G. Martinsson, and J. A. Tropp, "Finding structure with randomness: Probabilistic algorithms for constructing approximate matrix decompositions," *SIAM Review*, vol. 53, no. 2, pp. 217–288, 2011.

[15] B. McFee, *Digital Signals Theory, Spectral Leakage and Windowing*.

[16] M. Hasegawa-Johnson, "Short-time fourier transforms and filterbanks," Online: https://courses.physics.illinois.edu/ece417/fa2020/slides/lec05.pdf, 2020.

[17] S. M. Kuo, S. Mitra, and W. S. Gan, "Active noise control system for headphone applications," *IEEE Transactions on Control Systems Technology*, vol. 14, no. 2, pp. 331–335, 2006.

[18] "Aviation noise 2024 regional data.pdf," Noise — Federal Aviation Administration, https://www.faa.gov/sites/faa.gov/files/Aviation%20Noise%202024%20Regional%20Data.pdf.

[19] J. Ivošević, E. Ganić, A. Petošić, and T. Radišić, "Comparative uav noise-impact assessments through survey and noise measurements," *MDPI*, 2021.

[20] H. Davoren, "Naples airport considers relocation due to noise complaints, growth restrictions," GlobalAir.com, https://www.globalair.com/articles/naples-airport-considers-relocation-due-to-noise-complaints-growth-restrictions?id=6565, October 2023.

[21] "Lakeland airport working to cut down noise after complaints," BayNews9.com, https://baynews9.com/fl/tampa/news/2023/11/17/lakeland-airport-working-to-cut-down-noise-after-complaints.

[22] J. Simmons, "Responding to resident complaints, county will plan strategy to reduce airport noise," Observer Local News, https://www.observerlocalnews.com/news/2020/feb/03/responding-to-resident-complaints-county-will-plan-strategy-to-reduce-airport-noise/, 2020.

[23] T. Dbouk and D. Drikakis, "Quadcopter drones swarm aeroacoustics," *Physics of Fluids*, vol. 33, no. 5, p. 057112, 2021. [Online]. Available: https://pubs.aip.org/aip/pof/article-abstract/33/5/057112/1077384/Quadcopter-drones-swarm-aeroacoustics

Appendix

A Gavish Donoho Rank Approximation

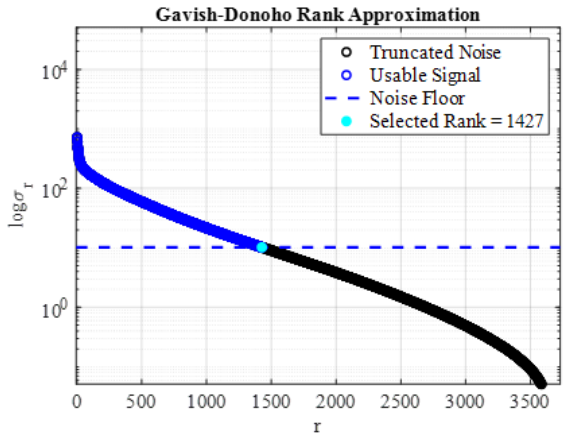

Figure 9: Evaluation of Noise Floor using Gavish-Donoho Rank Approximation Approach.

When more accurate compression results are required for analysis, the Gavish Donoho Rank Approximation can be used. This rank approximation is more computatyionlly expensicve but provides a very accurate low rank approximation. Single-value hard thresholding is used for rank reduction for economical SVD, the math for this process is described in https://arxiv.org/pdf/1305.5870 as an Optimal Singular Value Shrinker.

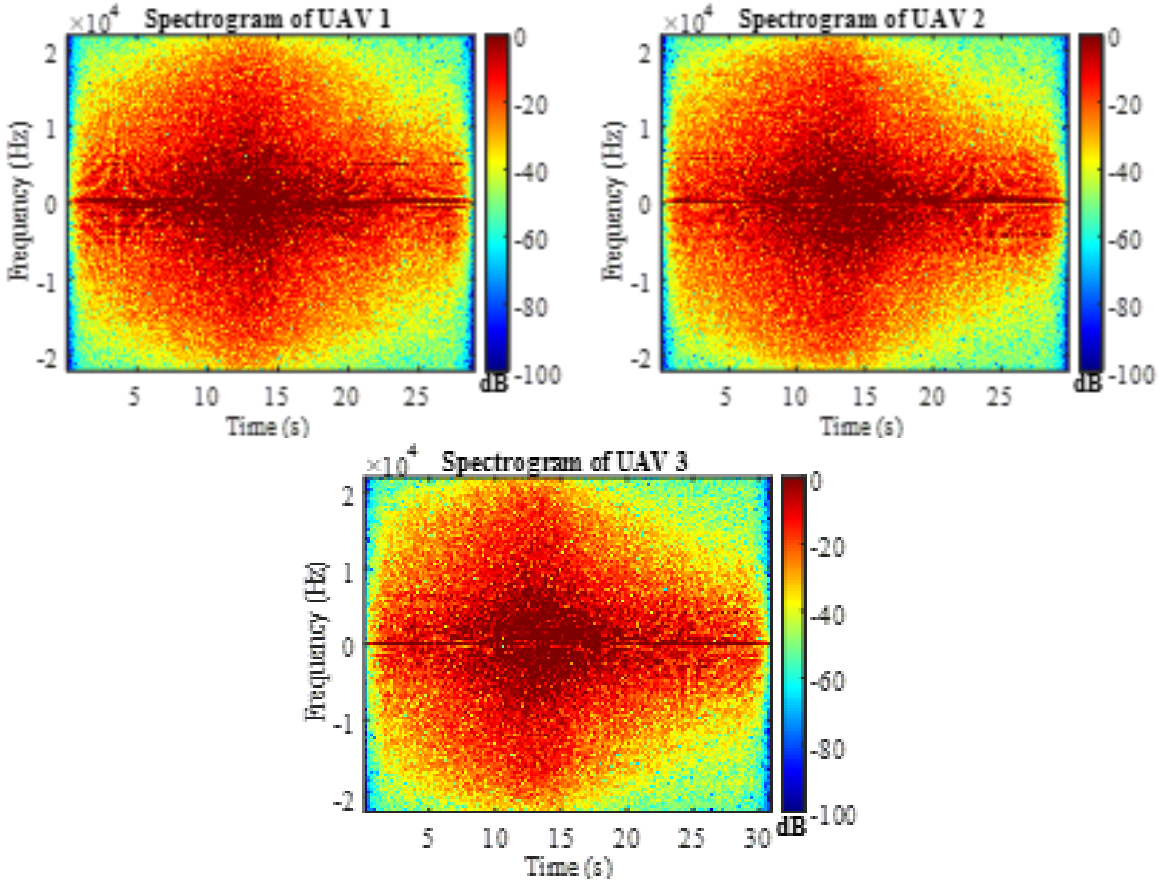

Figure 10: Spectogram of reconstructred UAV signals after applying Gavish-Donoho Rank Approximation.

B ANCIR 2024 noise complaint statistics for the Southern region

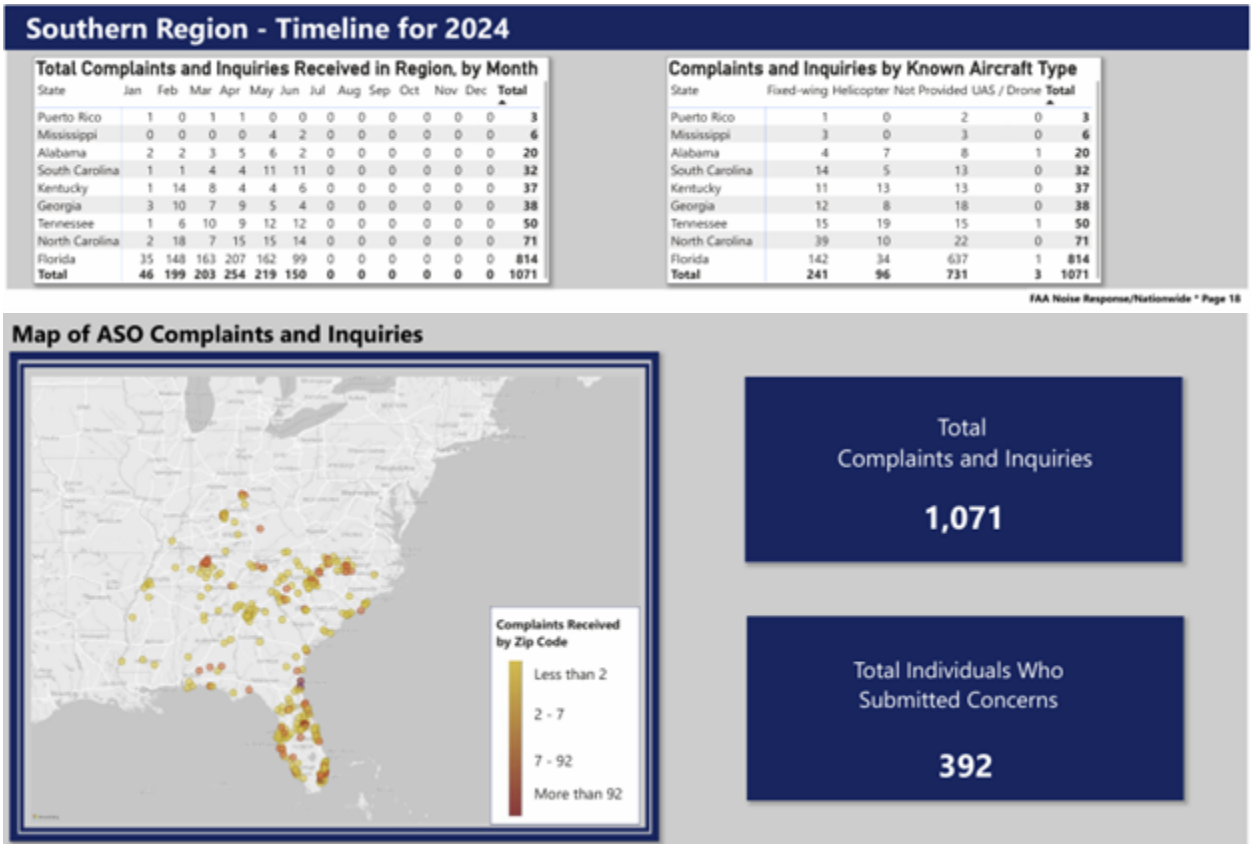

Figure 11: Visual Representations of complaint Statistics